Quantum Interference and Decoherence in Hexagonal Antidot Lattices

Yasuhiro Iye, Masaaki Ueki, Akira Endo and Shingo Katsumoto

Institute for Solid State Physics, University of Tokyo,
5-1-5 Kashiwanoha, Kashiwa, Chiba 277-8581 Japan

Abstract

The Altshuler-Aronov-Spivak (AAS) oscillations and the Aharonov-Bohm (AB) type oscillations both at low and high magnetic fields were observed in hexagonal antidot lattices fabricated from GaAs/AlGaAs two-dimensional electron gas sample. The periodicities in magnetic field and in gate bias voltage, of the high-field AB oscillation furnish information on the edge states localized around the antidots. The temperature dependences of these quantum oscillations are studied.

Study of Aharonov-Bohm (AB) effect constitutes one of the most powerful means to elucidate the phase-coherent properties of mesoscopic systems. It was initiated by observation of the Altshuler-Aronov-Spivak (AAS) oscillations with periodicity $h/2e$ in small metal cylinder[1], followed by observation of the AB oscillations with periodicity h/e in single metal rings[2]. These experiments were done in metallic systems where electron transport was diffusive. These effects were also observed in mesoscopic ring structures based on semiconductor two-dimensional gas (2DEG) systems where electron transport was in the ballistic or quasi-ballistic regime[3]. Analogous quantum osicllation phenomena were observed in 2DEG antidot lattices[4-6]. The AAS oscillation was observed in hexagonal antidot lattice[6]. The AB oscillation was observed in the commensurability resisitivity peak region of square antidot lattices[4,5].

It is known that the phase of the AB interference is sample specific, so that the AB amplitude diminishes in a system consisting of many nominally identical rings[7]. By contrast, the AAS effect, which originates from intereference of time-reversed pair of electron waves, is immune to such “ensemble averaging” effect. Therefore, the observation of the AB oscillation in antidot lattices of macroscopic size came as a bit of

surprise. Subsequent theoretical studies have attributed the effect to oscillatory fine structure of the density of state spectra, as calculated by periodic orbit theory[8]. Hence the effect is sometimes called AB-type oscillation to make distinction with the AB effect in single ring system. The details of the physical origin of the AB-type oscillation, however, remain to be worked out. In this work, we study the AAS and AB-type oscillations in hexagonal antidot lattices.

The samples were fabricated from a GaAs/AlGaAs 2DEG wafer with electron density $n = 3.6 \times 10^{15}\,\mathrm{m}^{-2}$ and mobility $\mu = 68\,\mathrm{m}^2/\mathrm{Vs}$. The hexagonal pattern of antidots was created on a Hall bar by electron beam lithography and wet chemical etching. The lattice parameter was $a = 960\mathrm{nm}$ and the aspect ratio d/a (d being the diameter of antidot) was 0.6 (sample #1) and 0.7 (#2). Due to the finite width of depletion region, the effective diameter d^* of the antidot is larger than the lithographical value. The values of resisitivity at zero magnetic field were$1.2\,\mathrm{k}\Omega$ (#1) and $3.9\,\mathrm{k}\Omega$ (#2). The active region of the Hall bar contains about 10^4 antidots. The electron density can be changed by a front gate. Magnetoresistance and Hall resistance were measured by a standard low frequency ac technique at dilution refrigerator temperatures in a 15 tesla magnet.

Figure 1 shows a magnetoresistance trace of sample #2 taken at 30mK. The top panel shows an expanded view of the trace in the low magnetic field range with the smooth background subtracted. The AAS ($h/2e = \phi_0/2$) oscillation around zero magnetic field and the AB-type ($h/e = \phi_0$) oscillation at somewhat higher fields are clearly identified. The periods of these oscillations are consistent with the unit cell area $\left(\sqrt{3}/2\right)a^2 = 0.80\,\mu\mathrm{m}^2$ of the hexagonal lattice . The bottom panel shows the oscillatory part of the magnetoresistance peak at around 4.8T, which corresponds to the Hall plateau transition between $\nu = 3$ and 2. The period of this high-field AB oscillation reflects the effective area $(\pi/4)d^{*2}$ of the antidots with appropriate allowance for the width of depletion region, indicating that these oscillations originate from the edge channels encircling the antidots. The single particle states localized around each antidot are quantized so as to enclose an integer number of flux quanta. As the magnetic field is swept, these single particle states pass through E_F one by one, leading to the AB oscillation.

Figure 2 shows the evolution of the high-field AB oscillation at $\nu \sim 2.5$ with the

gate voltage. The top panel shows the global evolution of the Fourier spectrum. The increase of the AB frequency with decreasing V_G is attributed to the increase of effective antidot area due to increasing depletion region. The bottom panel shows a gray scale plot of the AB oscillation at $B \sim 3.7\,\mathrm{T}$ ($\nu \sim 3.5$) and $V_G \sim 0\,\mathrm{mV}$. It is seen that the phase of the AB oscillation changes approximately linearly with V_G. The period ΔV_G, i.e. the change in V_G which gives rise to phase shift of one full cycle is 2.5mV for this figure. The evolution of the AB oscillation phase arises from the Fermi level shift with V_G given by $\Delta E_F = \alpha \Delta V_G$, where $\alpha \equiv \mathrm{d}E_F/\mathrm{d}V_G$ is a conversion factor experimentally determined by measuring the V_G-dependence of the carrier density. The conversion factor for the present sample was found to be $\alpha = 0.023$ for $V_G = 0\,\mathrm{mV}$ and $\alpha = 0.033$ for $V_G = -60\,\mathrm{mV}$ at which the data discussed below were taken. These values of α are in good agreement with the value $(C/e)(\pi\hbar^2/m) \approx 0.03$ calculated from a simple capacitance model.

Table 1 summarizes the values of ΔV_G together with those of the AB period $\Delta B = \phi_0/S$ of the high-field AB oscillation. It is noted that the value of ΔB is larger for higher magnetic field (lower filling factor) and smaller for more negative V_G. The former is attributed to the fact that, for higher field, the relevant edge channel (the outermost one) is that of lower Landau level and is closer to the antidot periphery. The latter is associated with the increase of effective area of antidots due to more extended depletion region for more negative gate bias. The periodicity in V_G becomes smaller for higher B and for more negative V_G. The latter feature, *i.e.* the difference in ΔV_G between $V_G = 0$ and $-60\,\mathrm{mV}$ in Table 1, is quantitatively explained when the difference in the conversion factor α for these values of V_G is taken into account. The former feature, the *B*-dependence of ΔV_G is linked to the fact that the difference in radius Δr of two adjacent single particle states is smaller for higher magnetic field, since it is given by $\Delta r = \phi_0/2\pi rB$. The single particle level spacing expressed as $\Delta E = (\mathrm{d}V/\mathrm{d}r)\Delta r = (\mathrm{d}V/\mathrm{d}r)(\phi_0/2\pi rB)$ is therefore smaller for higher magnetic field. Here $\mathrm{d}V/\mathrm{d}r$ represents the slope of the antidot potential in the radial direction. This is in line with the trend shown in Table 1. For quantitative understanding, however, the following factor should be taken into account . If we use $\mathrm{d}V/\mathrm{d}r \sim$ a few eV/μm obtained from rough estimate based on band bending in the depletion region, the level spacing becomes on the order of $\Delta E \approx$ a few meV for typical experimental conditions.

On the other hand the values of ΔV_{G} obtained are a few meV, which when translated to ΔE_{F} by the conversion factor α become on the order of a few tens μeV. This indicates that we have to use the effective value of $\mathrm{d}V/\mathrm{d}r$ with the self-consistent screening taken into account,. The relevant values of $\mathrm{d}V/\mathrm{d}r$ are much smaller than the slope of the bare antidot potential.

Figure 3 shows the temperature dependences of the amplitude of the three types of quantum oscillation, the AAS, low-field AB and high-field AB effects. The T-dependence of the AAS amplitude is governed by that of the phase coherence length $L_\phi \propto T^{-p}$. The two samples showed $A_{\mathrm{AAS}} \propto \exp\left(-(T/T^*_{\mathrm{AAS}})^p\right)$ with $p \approx 1.5$ (sample #1) and 1.1(#2). These values are intermediate between the $L_\phi \propto T^{-2}$ for 2D system and $L_\phi \propto T^{-1}$ for 1D system[9]. The phase coherence length L_ϕ as estimated from the ratios of the harmonic components is $L_\phi \approx 4-6\mu\mathrm{m}$, and saturates at the lowest temperatures. The saturation of the AAS oscillation at low temperatures is more conspicuous for large negative gate bias (lower carrier density).

The T-dependence of the low-field AB oscillation follows $A_{\mathrm{AB}} \propto \exp\left(-T/T^*_{\mathrm{AB}}\right)$ with the value of T^*_{AB} smaller for the larger aspect ratio sample. If the AB-type oscillation is considered as simple reflection of the oscillatory fine structure of a fixed density of state profile with characteristic energy scale ΔE, the expected temperature dependence is $\propto x/\sinh x$ with $x = 2\pi^2 k_{\mathrm{B}} T/\Delta E$, which saturates at low temperatures. The experimental result, however, indicates behavior closer to an exponential dependence. In the present system, the overall sample size is much larger than the phase coherence length L_ϕ, but the latter increases with decreasing temperature. This introduces an extra factor in temperature dependence through the ensemble averaging. The high-field AB oscillation also follows the exponential T-dependence, but with the values of T^*_{AB} smaller for higher magnetic fields.

In conclusion, we have observed three types of quantum oscillations, AAS, low-field AB and high-field AB effects, in macroscopic samples of hexagonal antidot lattice. The magnetic field and gate voltage dependences of the high-field AB oscillations reveal the characteristics of the localized states formed around the antidots. The basic mechanisms governing the temperature dependence of the quantum oscillations in macroscopic antidot lattices are yet to be worked out.

This work was supported by Grant-in-Aid for COE Research “Quantum Dot and Its

Application", and by Grant-in-Aid for Scientific Research #13304025 from the Ministry of Education, Culture, Sports, Science and Technology (MEXT), Japan.

References

[1] D.Yu.Sharvin and Yu.V.Sharvin, Pis'ma Zh. Eksp. Theor. Fiz. 34 (1981) 285. [JETP Lett. 34 (1981)272.]

[2] R.A.Webb, S.Washburn, C.P.Umbach and R.B.Raibowitz, Phys. Rev. Lett. 54 (1985).

[3] S.Datta, M.R.Mellock, S.Bandyopadhyay, R.Norem, M.Vazirir, M.Miller and R.Reifenberger, Phys. Rev. Lett. 55 (1985) 2344; G. Timp, A. M. Chang, J. E. Cunningham, T. Y. Chang, P. Mankiewich, R. Behringer, and R. E. Howard, Phys. Rev. Lett. 58 (1987) 2814.

[4] F.Nihey and K.Nakamura, Physica B184 (1993) 398

[5] D.Weiss, K.Richter, A.Menshing, R.Bergmann, H.Schewzer, K.von Klitzing and G.Weimann, Phys. Rev. Lett. 70 (1993) 4118.

[6] F.Nihey, S.W.Hwang and K.Nakamura, Phys. Rev. B51 (1995) 4649.

[7] C.P.Umbach, C.van Haesendonck, R.B.Laibowitz, S.Washburn and R.A.Webb, Phys. Rev. Lett. 56 (1986) 386.

[8] T.Ando, S.Uryu, S.Ishizaka and T.Nakanishi, Choas, Solitons & Fractals 8 (1997) 1057; T.Ando, in "Mesoscopic Physics and Electronics" eds. T.Ando et al. (Springer, 1998) p.72.

[9] J.J.Lin and J.P.Bird, J. Phys.: Condens. Matter 14 (2002) R501; A.E.Hansen, A.Kristensen, S.Pedersen, C.B.Sorensen and P.E.Lindelof, Phys. Rev. B64 (2001) 045327; K.Kobayashi, H. Aikawa, S. Katsumoto, and Y. Iye, J. Phys. Soc. Jpn. 71 (2002) 2094.

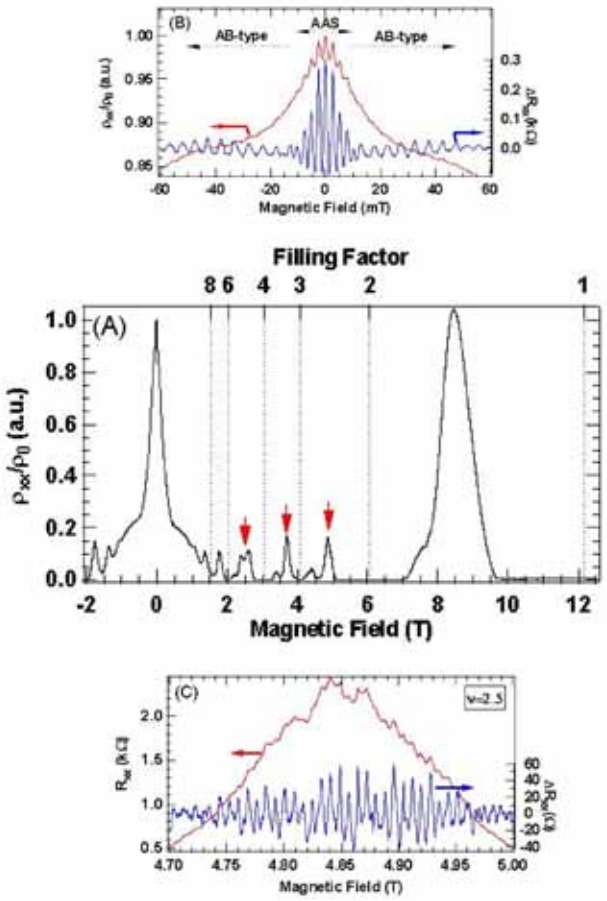

Fig.1 Magnetoresistance trace of a hexagonal antidot lattice. The upper panel shows the oscillatory part of the resistance at low magnetic fields, exhibiting the AAS ($h/2e$) and AB-type (h/e) oscillations. The lower panel shows the oscillatory part superposed on the resistance peak between $\nu = 3$ and 2.

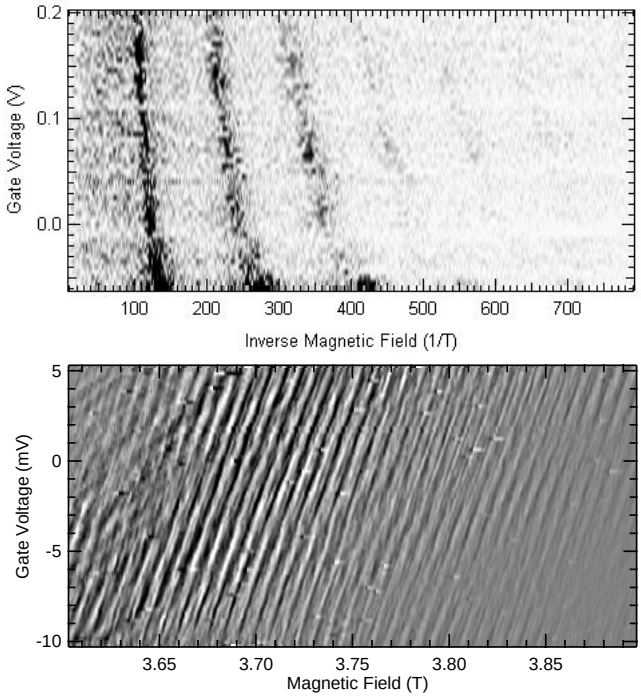

Fig.2 *Upper panel*: Global evolution of the Fourier spectrum of the high field AB oscillation at $\nu = 2.5$ with the gate voltage V_G.

Lower panel: Gray scale plot of the AB-type oscillation at $B \sim 3.7\,\mathrm{T}$ and $V_G \sim 0\,\mathrm{mV}$, showing the phase shift with V_G.

V_G (mV)	n_e ($10^{15}m^{-2}$)	B (T)	ν	ΔB (mT)	ΔV_G (mV)
0	2.9	1	12-10	5.7±0.9	6.3
		2.5	6-4	7.4±0.6	4.2
		3.7	4-3	7.9±0.4	2.5
		4.9	3-2	8.0±0.3	2.0
-60	2.4	3.4	~3	7.4±0.2	1.7

Table 1 Values of ΔB and ΔV_G for the high field AB oscillation in different regions of B and V_G.

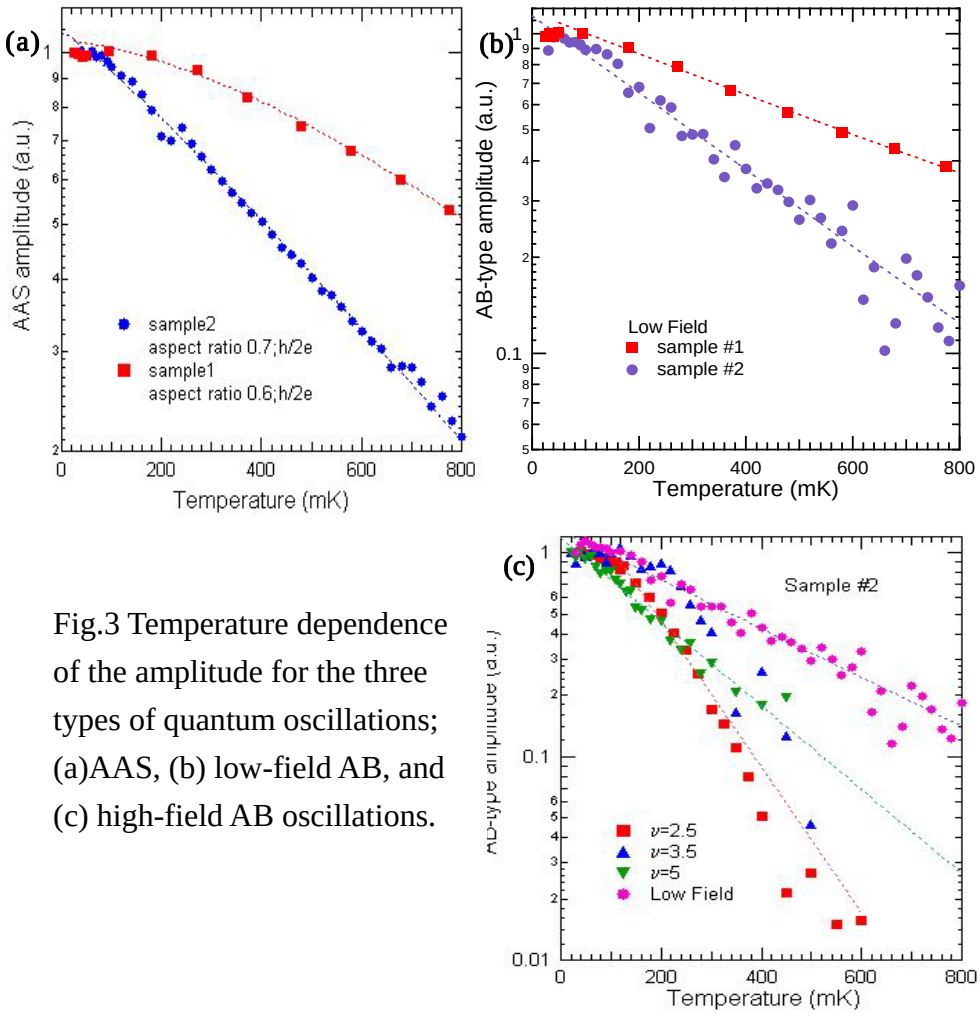

Fig.3 Temperature dependence of the amplitude for the three types of quantum oscillations; (a)AAS, (b) low-field AB, and (c) high-field AB oscillations.